

Gaussian-Based Parametric Bijections For Automatic Projection Filters

Muhammad F. Emzir, Zheng Zhao, Lahouari Cheded, Simo Särkkä

Abstract—The automatic projection filter is a recently developed numerical method for projection filtering that leverages sparse-grid integration and automatic differentiation. However, its accuracy is highly sensitive to the accuracy of the cumulant-generating function computed via the sparse-grid integration, which in turn is also sensitive to the choice of the bijection from the canonical hypercube to the state space. In this paper, we propose two new adaptive parametric bijections for the automatic projection filter. The first bijection relies on the minimization of Kullback–Leibler divergence, whereas the second method employs the sparse-grid Gauss–Hermite quadrature. The two new bijections allow the sparse-grid nodes to adaptively move within the high-density region of the state space, resulting in a substantially improved approximation while using only a small number of quadrature nodes. The practical applicability of the methodology is illustrated in three simulated nonlinear filtering problems.

Index Terms—projection filter, adaptive bijection, numerical quadrature, automatic differentiation, sparse-grid integration

I. INTRODUCTION

The projection filter [1], [2] is an approximate optimal filtering method based on projections of probability densities on manifolds. Specifically, the filter projects the Kushner–Stratonovich equation [3] of the optimal filtering solution onto a finite-dimensional manifold of parametric densities, producing a finite-dimensional stochastic differential equation (SDE) representation. When the manifold is the manifold formed by mixtures of probability densities and the L^2 metric is used, then the projection filter is equivalent to a Galerkin method for solving the Kushner–Stratonovich equation (see [4, Theorem 5.1]).

The projection filter has so far been used only in limited scenarios. Outside of the Gaussian family, the most prevalent applications have been in univariate dynamical systems [2], [5]–[7]. Recently, Emzir et al. [8] introduced an automatic projection filter for a wider class of filtering problems. Although the method is applicable to a large class of multivariate dynamical systems, its computational can be demanding for using a large number of quadrature nodes [8]. Using a large number of nodes is often needed because of the fixed (rather than an adaptive) bijection between the canonical hypercube and the integration domain. In the other way around, the fixed bijection also practically limits the numerical accuracy of the filter when the computational budget is limited.

In this study, we propose two bijections that transform the nodes of sparse-grid quadratures to adaptively cover the high-density domain of the projected conditional densities. The main challenge in constructing such bijections is found to be the impossibility of obtaining a bijection that transforms the integrand into a polynomial function in the transformed space, thereby achieving zero integration error (see Proposition 1). Further, we show that using squared integration error as an optimization cost function also leads to non-explicit bijection functions (see Proposition 2). To overcome these difficulties, in the first bijection, we minimize the Kullback–Leibler divergence between the projected conditional density and a Gaussian density via moment matching (see Proposition 3). Not only does this result in an explicit bijection form, but it also optimizes the squared integration error under certain technical conditions (see Proposition 4). We then adapt this technique to Gauss–Hermite quadrature.

When the automatic projection filter algorithm is combined with these bijections, the part of the state space which has a high filtering density can be automatically tracked. This improvement requires much fewer quadrature nodes than those using static bijections. We illustrate the effectiveness of the proposed bijections using three numerical examples where it is challenging to confine conditional densities inside a fixed domain. We also generalize the filtering problems in comparison to [8] by only requiring that the drift and diffusion functions belong to a vector space that is closed under partial differentiation.

The paper is organized as follows. We first review the projection filter for the exponential family in Section II, and then explain how to propagate the SDE parameters using numerical integration and automatic differentiation. Section III delivers the main contributions of the paper, which are the two new bijections from the canonical hypercube to the state space of the projection filter. Section IV shows the practical applicability of the bijections in the automatic projection filter in three simulated nonlinear filtering problems. Finally, Section V summarizes the results and concludes the paper.

II. AUTOMATIC PROJECTION FILTER

In this section, we review the relevant theoretical results that constitute the foundation of the automatic projection filter [8] and also to present the extension of the model considered in this paper. We consider optimal filtering problems on the following state-space model consisting of continuous-time stochastic dynamic and observation models:

$$dx_t = f(x_t) dt + \varrho(x_t) dW_t, \quad (1a)$$

$$dy_t = h(x_t) dt + dV_t, \quad (1b)$$

where $x_t \in \mathcal{X} := \mathbb{R}^d$, $y_t \in \mathcal{Y} := \mathbb{R}^{d_y}$. The processes $\{W_t, t \geq 0\}$ and $\{V_t, t \geq 0\}$ are independent Wiener processes taking values in \mathbb{R}^{d_w} and \mathbb{R}^{d_y} with invertible spectral density matrices Q_t and R_t for all $t \geq 0$, respectively. For the sake of exposition, and without a loss of generality, in the rest of the paper, we assume that $R_t = I$ for all $t \geq 0$.

The conditional probability density of the state at time t , space x_t , given a history of measurements y_τ , $0 \leq \tau \leq t$, satisfies the Kushner–Stratonovich equation [3]. Let us define a class of probability densities \mathcal{P} with respect to the Lebesgue measure on \mathcal{X} as $\mathcal{P} = \{p \in L^1 : \int_{\mathcal{X}} p(x) dx = 1, p(x) \geq 0, \forall x \in \mathcal{X}\}$. In particular, let us consider the exponential family

$$\text{EM}(c) := \left\{ p \in \mathcal{P} : p(x) = \exp\left(c(x)^\top \theta - \psi(\theta)\right) \right\}, \quad (2)$$

where $\theta \in \Theta \subset \mathbb{R}^m$ is the natural parameter and $c: \mathbb{R}^d \rightarrow \mathbb{R}^m$ is a vector of natural statistics that are assumed to be linearly independent. The natural parameter space Θ is defined as

$$\Theta := \left\{ \theta \in \mathbb{R}^m : \int_{\mathcal{X}} \exp\left(c(x)^\top \theta\right) dx < \infty \right\}. \quad (3)$$

An exponential family is said to be regular if Θ is an open subset of \mathbb{R}^m . In this work, we focus on regular exponential families. In the development of the proposed improved projection filter, we

extensively use the cumulant-generating function (i.e., the log Laplace transform or log partition function [8], [9]) defined by

$$\psi(\theta) = \log \left[\int_{\mathcal{X}} \exp(c(x)^\top \theta) dx \right], \quad \theta \in \Theta. \quad (4)$$

Because the exponential family is assumed to be regular and the natural statistics are linearly independent, the exponential family is minimal [10], [11]. We recall the following standard result for a minimal regular exponential family [10, Theorems 2.2.1 and 2.2.5].

Theorem 1. *In a regular exponential family, the set Θ as defined in (3) is convex. The cumulant-generating function $\psi(\theta)$ is strictly convex on Θ and it is differentiable up to an arbitrary order. The moments of the natural statistics $c_i(x)$, $i = 1, \dots, m$ exist for any order, and the expectations of c_i and the corresponding Fisher information matrix g are, respectively, given by,*

$$\mathbb{E}_\theta [c_i] = \frac{\partial \psi(\theta)}{\partial \theta_i}, \quad g_{i,j}(\theta) = \frac{\partial^2 \psi(\theta)}{\partial \theta_i \partial \theta_j}. \quad (5)$$

If the representation is minimal, then g is positive definite.

Let us denote by $\mathcal{S} = \{p_\theta : \theta \in \Theta \subseteq \mathbb{R}^m\}$ a class of parametric densities which does not have to be the exponential family. There are a few approaches that can be used to project the Kushner–Stratonovich equation onto the manifold of parametric densities [12]. The standard way is to leverage the property that the square root of the density $\sqrt{p_t}$ belongs to L^2 . Therefore, by requiring that the stochastic differential $d\sqrt{p_t}$ is an element of L^2 and by expressing the Kushner–Stratonovich equation in its Stratonovich form, we can project $d\sqrt{p_t}$ onto the tangent space $T_{\sqrt{p_\theta}} S^{1/2}$. This is elucidated in the following lemma [2, Lemma 2.1].

Lemma 1. *Let $p_\theta \in \mathcal{S}$, and u be a function such that $\mathbb{E}_{p_\theta}[|u|^2] < \infty$. Then the projection of $v := u\sqrt{p_\theta} \in L^2$ onto the tangent space $T_{\sqrt{p_\theta}} S^{1/2}$ is given by*

$$\Pi_\theta v = \sum_{i=1}^m \sum_{j=1}^m 4g_{ij}^{-1} \left\langle v, \frac{1}{2\sqrt{p_\theta}} \frac{\partial p_\theta}{\partial \theta_j} \right\rangle \frac{1}{2\sqrt{p_\theta}} \frac{\partial p_\theta}{\partial \theta_i}, \quad (6)$$

where the inner product is defined as $\langle u, v \rangle = \int u(x)v(x) dx$.

For the exponential family $\text{EM}(c)$, the projection filter using Stratonovich projection is given by [2]:

$$\begin{aligned} d\theta_t &= g(\theta_t)^{-1} \mathbb{E}_{\theta_t} \left[\mathcal{L}[c] - \frac{1}{2} h^\top h [c - \eta(\theta_t)] \right] dt \\ &\quad + g(\theta_t)^{-1} \sum_{k=1}^{d_y} \mathbb{E}_{\theta_t} [h_k [c - \eta(\theta_t)]] \circ dy_{t,k}. \end{aligned} \quad (7)$$

In the equation above, \mathbb{E}_θ is the expectation with respect to the parametric probability density p_θ , h_k is the k -th element of h , $\theta_t \mapsto \eta(\theta_t) := \mathbb{E}_{\theta_t}[c]$, \mathcal{L} is the backward Kolmogorov diffusion operator, and \circ denotes the Stratonovich multiplication.

We can now extend the class of state-space models considered in [8] as follows. Let \mathcal{P} be a set of smooth functions $\varphi: \mathbb{R}^d \rightarrow \mathbb{R}$ such that \mathcal{P} is a finite-dimensional vector space that is closed under partial differentiation with respect to x_1, \dots, x_d . Examples of sets \mathcal{P} are polynomials on x_1, \dots, x_d with a total order less or equal to some $k \in \mathbb{N}$ and functions of the form $f(x) = \sum_{j=1}^{n_k} a_j \cos(k_j^\top x) + b_j \sin(\ell_j^\top x)$, with $a_j, b_j \in \mathbb{R}$, $k_j, \ell_j \in \mathbb{Z}^d$, and $n_k \in \mathbb{N}$. We use the following assumptions on the model (1).

Assumption 1. *Elements of functions f, h , and $q\theta^\top$ belong to \mathcal{P} .*

Assumption 2. *The natural statistics $\{c_i\}$ are selected as linearly independent elements of \mathcal{P} .*

Assumption 3. *Each element of h is in the span of $\{1, c_1, \dots, c_m\}$. This means there exists $\lambda_k \in \mathbb{R}^{d_y}$ for $k = 0, \dots, m$, such that $h = \lambda_0 + \sum_{k=1}^{d_y} \lambda_k c_k$.*

Under Assumption 3, the resulting exponential family of probability densities is known as the $\text{EM}(c^*)$ family [2]. For this specific family, the projection filter equation reduces to [2, Theorem 6.3]

$$d\theta_t = g(\theta_t)^{-1} \mathbb{E}_{\theta_t} \left[\mathcal{L}[c] - \frac{1}{2} (h^\top h) [c - \eta(\theta_t)] \right] dt + \sum_{k=1}^{d_y} \lambda_k dy_{t,k}, \quad (8)$$

Assumptions 1 and 2 ensure that every element of $\{\mathcal{L}[c], h^\top h, h^\top h c\}$ belongs to a larger vector space \mathcal{P} spanned by the basis of \mathcal{P} and a finite number of multiplications of basis functions of \mathcal{P} . Explicitly, we can write $\mathcal{L}[c] - \frac{1}{2} (h^\top h) c = a_0 + A_0 \tilde{c}$ and $\frac{1}{2} (h^\top h) = b_0 + b_h^\top \tilde{c}$, where $a_0 \in \mathbb{R}^m$, $A_0 \in \mathbb{R}^{m \times (m+m_h)}$, $b_0 \in \mathbb{R}$, $b_h \in \mathbb{R}^{(m+m_h)}$, and $\tilde{c}^\top = [c^\top, c_h^\top]$. Note that $c_h: \mathbb{R}^d \rightarrow \mathbb{R}^{m_h}$ is the vector of the remaining statistics of x that are linearly independent of the elements of c . Therefore, under these assumptions, Equation (8) can be expressed as

$$d\theta_t = g(\theta_t)^{-1} [a_0 + b_0 \eta(\theta_t) + M(\theta_t) \tilde{\eta}(\theta_t)] dt + \lambda dy_t, \quad (9)$$

where $\lambda = [\lambda_1, \dots, \lambda_m]^\top$, $M(\theta_t) = A_0 + \eta(\theta_t) b_h^\top$, and $\tilde{\eta}(\theta_t) := \mathbb{E}_{\theta_t}[\tilde{c}]$.

In order to solve (9), we need to compute the expectation $\tilde{\eta}$ and the Fisher metric g . In the automatic projection filter [8], the Fisher metric g is obtained by automatic differentiation of the approximated cumulant-generating function via Theorem 1. The cumulant-generating function can be approximated via Gauss–Chebyshev quadrature in the univariate case or via sparse-grid integration methods in the multivariate case. For the expected values of the extended statistics $\tilde{\eta}$, the automatic projection filter uses the following lemma to calculate the remaining expectations in (9) [8, Proposition 5.2].

Lemma 2. *Let $s(x): \mathbb{R}^d \rightarrow \mathbb{R}$ be a statistic, linearly independent of the natural statistics $c(x)$. If there exists an open neighborhood about the zero Θ_0 such that for $\tilde{c} := [c^\top(x) s(x)]^\top$, the quantity $\tilde{\psi}(\tilde{\theta}) := \log \left(\int_{\mathcal{X}} \exp(\tilde{c}^\top \tilde{\theta}) dx \right) < \infty$ for any $\tilde{\theta} \in \Theta \times \Theta_0$, then for any $\theta \in \Theta$*

$$\mathbb{E}_\theta[s] = \frac{\partial \tilde{\psi}(\tilde{\theta})}{\partial \tilde{\theta}_{m+1}} \Big|_{\tilde{\theta}=\theta_*}, \quad \theta_* = \begin{bmatrix} \theta \\ 0 \end{bmatrix}.$$

III. ADAPTIVE PARAMETRIC BIJECTIONS

In this section, we present the key contributions of this paper. Before doing so, let us first see the difficulties for adopting a static bijection, as was done in [8].

A. Challenges of static bijection

Although the automatic projection filter has been shown to perform well with multivariate dynamics [8], it unfortunately requires a large number of quadrature nodes. This is due to the need for the accurate computation of the exponential of the cumulant-generating function (4), which is done via numerical integration. To compute the cumulant-generating function for a parametric density p_θ a fixed smooth bijection $\phi: \mathcal{D} \rightarrow \mathcal{X}$ is used, where $\mathcal{D} := (-1, 1)^d$ is the canonical hypercube. Because during filtering, the high-density region of the filtering density moves within \mathbb{R}^d , fixing the bijection can lead to numerical instabilities. To illustrate this, let us denote by $\tilde{X} = \{\tilde{x}_i\}_{i=1}^N$ the set of quadrature nodes in the canonical hypercube and consider the univariate case with $p_\theta(x) = \frac{1}{\sqrt{2\pi}} \exp(-(x - \theta)^2/2)$ and $\phi = \tanh^{-1}(\tilde{x})$. In the domain \mathcal{D} , when a substantial part of

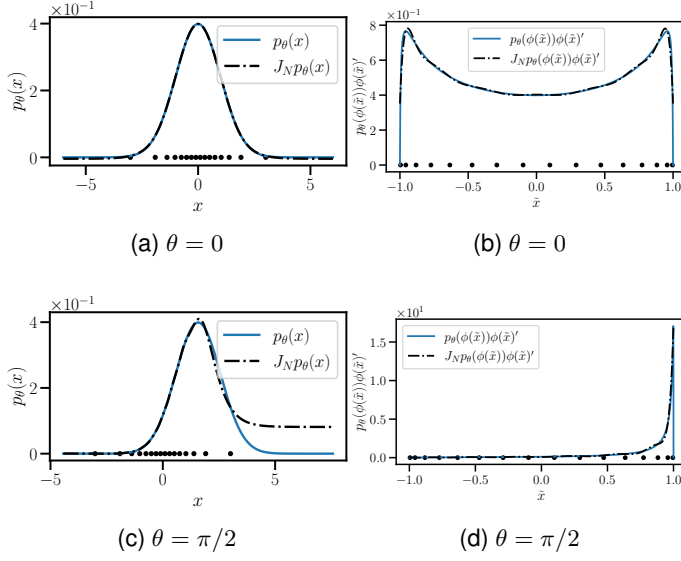


Fig. 1. Illustration of 16 bijected Gauss–Chebyshev's quadrature nodes, parametric density p_θ , and interpolated approximation using Chebyshev's nodes with the bijection $\phi = \tanh^{-1}$. Figs. (a) and (c) are in the original sample space \mathcal{X} and Figs. (b) and (d) are in the bijected sample space $\phi(\mathcal{X})$. When θ is shifted quite far from zero, the quadrature nodes do not entirely cover most of the high-density region of p_θ .

the bijected nodes $\phi(\tilde{x})$ lies outside the high-density interval, the function $\phi'(\tilde{x}) p_\theta(\phi(\tilde{x}))$ moves to edge of \mathcal{D} , and is almost zero at the other edge. Fig. 1 illustrates this effect with θ being either 0 or $\pi/2$, and by using only 16 quadrature nodes, $\{\phi(\tilde{x}_i)\}$ does not cover the region of high p_θ value as θ moves away from zero. Even worse, when θ is far from zero, increasing the number of quadrature nodes does not noticeably decrease the integration error. We show how to address this problem in the next section.

B. First Gaussian-Based Parametric Bijection

The aforementioned challenges motivates us to propose a new parametric bijection ϕ_ξ , where the bijection parameter $\xi \in \mathbb{R}^{n_\xi}$, $n_\xi \in \mathbb{N}$ can be used to reduce the numerical integration error. Let us first consider the univariate case and introduce a parametric probability density q_ξ with support \mathbb{R} . Then $\zeta_\xi(x) := 2 \int_{-\infty}^x q_\xi(y) dy - 1$ is a valid bijection from $\mathbb{R} \rightarrow \mathcal{D}$.

Now let us choose an exponential family manifold with m natural parameters. Choosing $\phi_\xi = \zeta_\xi^{-1}$, we can rewrite the exponential of the cumulant-generating function as

$$\exp(\psi(\theta)) = \int_{\mathcal{D}} \exp(c(\phi(\tilde{x}))^\top \theta) \frac{1}{2q_\xi(\phi(\tilde{x}))} d\tilde{x}. \quad (10)$$

Instead of directly numerically computing this function using its definition (4), it is beneficial to use this transformed integral representation instead. The accuracy of the quadrature approximation to this integral depends on the choice of q_ξ . Recall that a Gaussian quadrature rule with N quadrature nodes is exact when the integrand is chosen to be a polynomial of order $2N - 1$ or less [13]. Therefore, in order to get an accurate integration result, we can choose a q_ξ such that the integrand is close to a polynomial of order $2N - 1$ or less. In fact, if we chose q_ξ to be exactly p_θ , then we would have the integrand equal to $\frac{1}{2} \exp(\psi(\theta))$. This would mean that the integration result would be exact, thus avoiding any integration errors. However, in the following proposition we show that there is no such

a bijection that can be evaluated explicitly and makes the integrand in (10) a polynomial.

Proposition 1. Let ϕ be a bijection from \mathcal{D} to \mathbb{R} and let $\text{EM}(c)$ be the exponential family given by (2) with parameters $\theta \in \Theta$, where Θ is given by (3). If there is no explicit antiderivative for $\beta(x) := \exp(c(x)^\top \theta)$ as a function of x , then there is no explicit bijection ϕ such that $\beta(\phi(\tilde{x})) \phi(\tilde{x})'$ is a polynomial of \tilde{x} .

Proof. Suppose $\beta(\phi(\tilde{x})) \phi(\tilde{x})' = \rho_n(\tilde{x})$, where ρ_n is a polynomial of order n in \tilde{x} . Integrating both sides gives

$$\lim_{s_* \downarrow -1} \int_{s=s_*}^{\tilde{x}} \beta(\phi(s)) \frac{d\phi(s)}{ds} ds = \lim_{s_* \downarrow -1} \int_{s=s_*}^{\tilde{x}} \rho_n(s) ds,$$

$$\lim_{s_* \downarrow -1} \int_{\phi=\phi(s_*)}^{\phi(\tilde{x})} \beta(\phi) d\phi = \int_{s=-1}^{\tilde{x}} \rho_n(s) ds = \bar{\rho}_n(\tilde{x}),$$

where $\bar{\rho}_n$ is a polynomial because ρ_n is. Since the antiderivative of β has no explicit form, there is no explicit form for ϕ neither. \square

Even if the explicit antiderivative of $\beta(x)$ does exist, that is, $\int \beta(x) dx = \bar{\beta}(x) + C$, then solving for the bijection ϕ might still be impossible as $\bar{\beta}(\phi)$ might not be invertible. Therefore, instead of aiming at zero integration error, we focus on finding a parametric bijection, or a family of them, which leads to a smaller integration error. For this purpose, let us use a d -dimensional numerical quadrature with a positive weight function $\omega(\tilde{x})$ and with N quadrature nodes as

$$Q_N^{d,\omega} g := \int_{\mathcal{D}} g(\tilde{x}) \omega(\tilde{x}) d\tilde{x} \approx \sum_{i=1}^N w_i g(\tilde{x}_i), \quad (11)$$

where \tilde{x}_i are the nodes and w_i are the weights of the quadrature rule. The weighting function $\omega(\tilde{x})$ varies for different quadrature schemes. It is well-known that for a univariate Gauss-type quadrature, the quadrature nodes are distinct, and the weights $\{w_i\}_{i=1}^N$ are positive [13, Theorem 1.46]. As a generalization of one-dimensional bijection ϕ_ξ , where $\frac{\partial \phi_\xi}{\partial \tilde{x}} = (2q_\xi(x))^{-1}$, in multivariate context, the bijection operator (also denoted as ϕ_ξ) is constructed from q_ξ , where $|\det \frac{\partial \phi_\xi}{\partial \tilde{x}}| = (2^d q_\xi(x))^{-1}$. By using the quadrature rule, we can approximate the expectation of an arbitrary function $f(x)$ with respect to the density p_θ by

$$\mathbb{E}_{\theta,N}[f; \xi] := Q_N^{d,\omega} [f(\phi_\xi) u(\phi_\xi) \omega^{-1}] \quad (12)$$

where $u(x) := p_\theta(x)/(2^d q_\xi(x))$.

The operator $f \mapsto \mathbb{E}_{\theta,N}[f; \xi]$ is linear, but it does not guarantee that $\mathbb{E}_{\theta,N}[1; \xi] = 1$. The following lemma lists four important properties of this operator that we will use in the subsequent developments.

Lemma 3. If the approximation of the cumulant-generating function using N quadrature nodes is given by $\psi(\theta)^{(N)} = \log(Q_N^{d,\omega} [\exp(c(\phi_\xi)^\top \theta) |\det \frac{\partial \phi_\xi}{\partial \tilde{x}}| \omega^{-1}])$, then the following hold:

- 1) $\mathbb{E}_{\theta,N}[1; \xi] = \frac{\exp(\psi(\theta)^{(N)})}{\exp(\psi(\theta))}$,
- 2) $\frac{\partial \psi(\theta)^{(N)}}{\partial \theta_j} = \frac{\mathbb{E}_{\theta,N}[c_j; \xi]}{\mathbb{E}_{\theta,N}[1; \xi]}$,
- 3) $\frac{\partial^2 \psi(\theta)^{(N)}}{\partial \theta_j \partial \theta_k} = \frac{\mathbb{E}_{\theta,N}[c_j c_k; \xi]}{\mathbb{E}_{\theta,N}[1; \xi]} - \frac{\mathbb{E}_{\theta,N}[c_j; \xi]}{\mathbb{E}_{\theta,N}[1; \xi]} \frac{\mathbb{E}_{\theta,N}[c_k; \xi]}{\mathbb{E}_{\theta,N}[1; \xi]}$,
- 4) $\frac{\mathbb{E}_{\theta,N}[f; \xi]}{\mathbb{E}_{\theta,N}[1; \xi]} = \sum_{i=1}^N w_i f(\phi_\xi(\tilde{x}_i)) \times \exp(c(\phi_\xi(\tilde{x}_i)^\top \theta - \psi(\theta)^{(N)})) \left| \det \frac{\partial \phi_\xi}{\partial \tilde{x}} \right| \omega(\tilde{x}_i)^{-1}$.

Proof. For the first equality, using the definition (12), we get:

$$\begin{aligned}\mathbb{E}_{\theta,N}[1;\xi] &= Q_N^{d,\omega} \left[u(\phi_\xi) \omega^{-1} \right], \\ &= Q_N^{d,\omega} \left[\exp \left(c(\phi_\xi)^\top \theta - \psi(\theta) \right) \left| \det \frac{\partial \phi_\xi}{\partial \tilde{x}} \right| \omega^{-1} \right] \\ &= \frac{\exp(\psi(\theta)^{(N)})}{\exp(\psi(\theta))}.\end{aligned}$$

The second and third equalities follow directly by taking derivatives of $\psi(\theta)^{(N)}$ with respect to θ_j , and with respect to θ_j and θ_k . The fourth equality follows from the first. \square

A natural way to choose the parameter ξ is by minimizing the square of numerical integration error of (10), that is, $(\exp(\psi(\theta)) - \exp(\psi(\theta)^{(N)}))^2$. Let us define the integration error $E_N[f(x);\xi]$ as follows:

$$E_N[f;\xi] := \mathbb{E}_\theta[f] - \mathbb{E}_{\theta,N}[f;\xi]. \quad (13)$$

Then, since $\exp(\psi(\theta)) - \exp(\psi(\theta)^{(N)}) = \exp(\psi(\theta))(1 - \mathbb{E}_{\theta,N}[1;\xi])$, minimizing the square of the numerical integration error of (10) is equivalent to minimizing $E_N[1;\xi]^2$. The following proposition gives a necessary and sufficient condition such that the squared error $E_N[1;\xi]^2$ is a convex function. We denote the partial ordering of two squared matrices as $A \succeq B$ if $A - B$ is a positive semidefinite matrix.

Proposition 2. Let $u(x) = \frac{p_\theta(x)}{2^d q_\xi(x)}$, where $q_\xi = \exp(\tilde{c}(x)^\top \xi - \psi(\xi))$, $c(x)$ and $\tilde{c}(x) \in \mathcal{C}^2(\mathbb{R})$ are the natural statistics of p_θ and q_ξ , respectively, $\psi(\xi)$ is the cumulant-generating function corresponding to q_ξ , and ϕ_ξ is a smooth bijection from \mathcal{D} to \mathbb{R}^d constructed from q_ξ . Also, let $\Xi := \{\xi \in \mathbb{R}^{n_\xi} : \psi(\xi) < \infty\}$. Then $E_N[1;\xi]^2$ is convex on an open convex set $\Xi_0 \subseteq \Xi$, if and only if for any $\xi \in \Xi_0$, the following condition is satisfied:

$$\mathbb{E}_{\theta,N} \left[\frac{1}{u} \frac{du}{d\xi}; \xi \right] \mathbb{E}_{\theta,N} \left[\frac{1}{u} \frac{du}{d\xi}; \xi \right]^\top \succeq E_N[1;\xi] \mathbb{E}_{\theta,N} \left[\frac{1}{u} \frac{d^2 u}{d\xi^2}; \xi \right]. \quad (14)$$

Proof. Using the definitions of $E_N[1;\xi]$ and $\mathbb{E}_{\theta,N}[\cdot]$ from (13) and (12) respectively, we can write

$$\frac{1}{2} \frac{\partial E_N[1;\xi]^2}{\partial \xi} = -E_N[1;\xi] \mathbb{E}_{\theta,N} \left[\frac{1}{u} \frac{du}{d\xi}; \xi \right] \quad (15)$$

and

$$\begin{aligned}\frac{1}{2} \frac{\partial^2 E_N[1;\xi]^2}{\partial \xi^2} &= \mathbb{E}_{\theta,N} \left[\frac{1}{u} \frac{du}{d\xi}; \xi \right] \mathbb{E}_{\theta,N} \left[\frac{1}{u} \frac{du}{d\xi}; \xi \right]^\top \\ &\quad - E_N[1;\xi] \mathbb{E}_{\theta,N} \left[\frac{1}{u} \frac{d^2 u}{d\xi^2}; \xi \right].\end{aligned} \quad (16)$$

Therefore, if for any $\xi \in \Xi_0$, condition (14) is satisfied, then $\frac{\partial^2 E_N[1;\xi]^2}{\partial \xi^2}$ is positive semidefinite. By [14, Theorem 4.5] $E_N[1;\xi]^2$ is a convex function on Ξ_0 . The necessary part can be obtained using a similar argument to the proof of [14, Theorem 4.5]. \square

We can now highlight two difficulties of using gradient-based method to find the minimizer of $E_N[1;\xi]^2$. First, by parts 1) and 4) of Lemma 3, the Jacobian and Hessian of $E_N[1;\xi]^2$ with respect to ξ , which are given respectively by (15) and (16), cannot be explicitly calculated unless the cumulant-generating function $\psi(\theta)$ is known in a closed form. Secondly, it is impossible to ensure the criterion that $E_N[1;\xi]^2$ is locally convex even on some bounded interval since its Hessian cannot be evaluated. As a consequence, using gradient methods or (quasi-)Newton methods for finding a locally optimal ξ is not feasible.

With that being said, a more promising approach is to select ξ such that q_ξ covers the high-density area of p_θ as tightly as possible by optimizing another criterion as explained below, and the resulting bijection ϕ_ξ should then be amenable to direct computation. This turns out to be a viable approach to take, and the thus-constructed bijection could be shown to work in practice as well as be optimal with respect to the squared integration error, under some technical conditions. Our starting point is the following lemma [15].

Lemma 4. Let q_ξ be a density from an exponential family with natural statistics given by $\tilde{c}(x)$. For any distribution p , the distribution q_ξ^* that minimizes $KL(p||q_\xi)$, satisfies

$$\mathbb{E}_{q_\xi^*}[\tilde{c}] = \mathbb{E}_p[\tilde{c}]. \quad (17)$$

Essentially, the exponential density q_ξ that minimizes the $KL(p||q_\xi)$ distance satisfies the moment-matching equality (17). If we choose q_ξ to be a Gaussian density, then the mean μ and variance Σ of q_ξ should satisfy

$$\mu_i = \mathbb{E}_\theta[x_i], \quad i = 1, \dots, d, \quad (18a)$$

$$\Sigma_{ij} = \mathbb{E}_\theta[(x_i - \mu_i)(x_j - \mu_j)], \quad i, j = 1, \dots, d. \quad (18b)$$

In the actual implementation, we replace the cumulant-generating function by its approximation $\psi(\theta)^{(N)}$ that is obtained from numerical integration using N quadrature nodes. Since the approximation errors of the parameters μ and Σ , as well as the cumulant-generating function $\psi(\theta)$, depend linearly on the integration errors on $\int \exp(c^\top x) dx$, then selecting an N such that all the approximation errors for μ , Σ , and $\psi(\theta)$ are simultaneously kept below their acceptable upper limits, is feasible (see [8, Theorem 3.1]).

In the following proposition, we show how to construct a smooth bijection ζ_ξ from \mathbb{R}^d to \mathcal{D} using a parametric density q_ξ . We also show that its inverse $\phi_\xi = \zeta_\xi^{-1}$ can be expressed in a closed form when using Gaussian density q_ξ with parameters in (18).

Proposition 3. Let $s: \mathbb{R}^d \times \mathcal{P} \rightarrow \mathcal{D}$ defined by

$$s(z, q_\xi) = \begin{bmatrix} s_1(z_1, q_\xi) \\ \vdots \\ s_d(z_d, q_\xi) \end{bmatrix}, \quad (19a)$$

$$s_i(z_i, q_\xi) = 2 \frac{\int_{-\infty}^{z_i} q_\xi(z_1, \dots, y_i, \dots, z_d) dy_i}{\int_{-\infty}^{\infty} q_\xi(z_1, \dots, y_i, \dots, z_d) dy_i} - 1. \quad (19b)$$

If q_ξ is a smooth density with support equal to \mathbb{R}^d , then $s(\cdot, q_\xi)$ is a smooth bijection from \mathbb{R}^d onto \mathcal{D} .

Assume that q_ξ is a Gaussian density with mean μ and covariance matrix $\Sigma \succ 0$, and let the eigendecomposition of Σ be given by $\Sigma = T^{-1} \Lambda T$, where T is unitary. Let \tilde{q}_ξ be another Gaussian density with mean at $T\mu$ and variance Λ . Define $\zeta_\xi: \mathbb{R}^d \rightarrow \mathcal{D}$ as $\zeta_\xi(x) = s(Tx, \tilde{q}_\xi)$. Then $\left| \det \frac{\partial \zeta_\xi}{\partial x} \right| = 2^d q_\xi$. Moreover, the inverse of ζ_ξ , denoted as $\phi_\xi: \mathcal{D} \rightarrow \mathbb{R}^d$, is given by

$$\phi_\xi(\tilde{x}) = \mu + \sqrt{2} T^{-1} \Lambda^{1/2} \text{erf}^{-1}(\tilde{x}), \quad \tilde{x} \in \mathcal{D} \quad (20)$$

where $\text{erf}^{-1}(\tilde{x}) = [\text{erf}^{-1}(\tilde{x}_1), \dots, \text{erf}^{-1}(\tilde{x}_d)]^\top$.

Proof. Each $s_i(z_i, q_\xi)$ is a smooth bijection from \mathbb{R} to $(-1, 1)$. By the definition of s , for each $\tilde{x} \in \mathcal{D}$ there exists $z \in \mathbb{R}^d$ such that $s(z, q_\xi) = \tilde{x}$. Let $z, y \in \mathbb{R}^d$, and suppose $s(z, q_\xi) = s(y, q_\xi)$. Since $s_i(z_i, q_\xi)$ is a smooth bijection, z_i must equal to y_i , which leads to $z = y$. The smoothness of ζ_ξ follows from that of $s_i(z_i, q_\xi)$ for each i .

For the second part, it can be verified that with $z = Tx$ and $\mu_z = T\mu$ we have $s_i(z_i, \tilde{q}_\xi) = \text{erf}(\frac{\Lambda_{ii}^{-1/2}(z_i - \mu_{z,i})}{\sqrt{2}})$.

Then since T is unitary, we get $\left| \det \frac{\partial \zeta_\xi}{\partial x} \right| = \left| \det \frac{\partial s(z, \bar{q}_\xi)}{\partial z} \right| = \prod_{i=1}^d 2 \frac{1}{\sqrt{2\pi\Lambda_{ii}}} \exp\left(-\frac{1}{2}(z_i - \mu_{z,i})^2\right) = 2^d q_\xi$. The inverse of ζ_ξ can be obtained directly from the definition of s_i \square

Proposition 3 tells us that for any non-degenerate Gaussian density q_ξ , there exists a bijection ζ_ξ such that the transformation of an infinitesimal volume dx on \mathbb{R}^d under ζ_ξ is equivalent to $2^d q_\xi$ times $d\tilde{x}$. The bijection ϕ_ξ given by (20) can be interpreted as the following consecutive operations. First it transforms the quadrature nodes from the canonical hypercube to \mathbb{R}^d by the inverse error function, then it scales each axis by the appropriate square roots of the eigenvalues of Σ . Afterwards, it rotates the quadrature nodes according to the unitary matrix T . Lastly it shifts the quadrature nodes by μ from the origin; see the middle columns of Figures 4 for an illustration of these operations. In the numerical implementation, we will use this bijection to project the Gauss–Chebyshev nodes (for univariate case), or the sparse Gauss–Patterson nodes (for multivariate case), from \mathcal{D} to \mathbb{R}^d (see [16] for details). We will refer to these numerical integrations as the Gauss–Chebyshev quadrature (GCQ) and the Gauss–Patterson quadrature (GPQ), respectively.

Let us turn our attention to checking if the parameters ξ that are selected via the moment-matching rule (17) also optimize $E_N[1; \xi]^2$ locally. Proposition 4 below shows that if we use an approximated version of the moment-matching criterion (17) for a general exponential family $\text{EM}(\tilde{c})$ (it does not have to be a Gaussian family), then the selected parameters ξ also optimize $E_N[1; \xi]^2$ under certain constraints in the numerical expectation. Explicitly, in a special case where both natural statistics c and \tilde{c} are equivalent, this constraint requires that the numerical expectation $\mathbb{E}_{N,\theta}[c; \xi] / \mathbb{E}_{N,\theta}[1; \xi]$ is equal to the true value of $\mathbb{E}_\theta[c]$.

Proposition 4. Let q_ξ in (19a) be a density from $\text{EM}(\tilde{c})$ where the natural statistics $\tilde{c}_i \in \mathcal{C}^2(\mathbb{R}^d)$ are linearly independent. The parameter ξ optimizes $E_N[1; \xi]^2$ if $\frac{\partial \psi(\xi)}{\partial \xi} - \frac{\mathbb{E}_{\theta,N}[\tilde{c}; \xi]}{\mathbb{E}_{\theta,N}[1; \xi]} + \frac{\mathbb{E}_{\theta,N}[\frac{dx}{d\xi} \frac{dm}{d\xi}; \xi]}{\mathbb{E}_{\theta,N}[1; \xi]} = 0$, where $m(\xi) := c^\top(x(\xi))\theta - \tilde{c}^\top(x(\xi))\xi - (\psi(\theta) - \psi(\xi))$. In particular, if the following approximated moment-matching rule is used to choose the parameter ξ :

$$\frac{\mathbb{E}_{\theta,N}[\tilde{c}; \xi]}{\mathbb{E}_{\theta,N}[1; \xi]} = \frac{\partial \psi(\xi)}{\partial \xi}, \quad (21)$$

then, the selected parameter ξ is a local optimum of $E_N[1; \xi]^2$ if $\mathbb{E}_{\theta,N}[\frac{dx}{d\xi} \frac{dm}{d\xi}; \xi] = 0$. If $\tilde{c} = c$ and $\xi = \theta$, then ξ is a local optimum of $E_N[1; \xi]^2$.

Proof. Let us denote $x(\xi) := \phi_\xi(\tilde{x})$. Using (15) from the proof of Proposition 2, we can write

$$\begin{aligned} \frac{1}{2\mathbb{E}_{\theta,N}[1; \xi]} \frac{dE_N[1; \xi]^2}{d\xi} &= - \left[\frac{\partial \psi(\xi)}{\partial \xi} - \frac{\mathbb{E}_{\theta,N}[\tilde{c}; \xi]}{\mathbb{E}_{\theta,N}[1; \xi]} \right. \\ &\quad \left. + \frac{\mathbb{E}_{\theta,N}[\frac{dx}{d\xi} \frac{dm}{d\xi}; \xi]}{\mathbb{E}_{\theta,N}[1; \xi]} \right] E_N[1; \xi]. \end{aligned}$$

Hence, if the approximated moment-matching rule (21) is satisfied, and $\mathbb{E}_{\theta,N}[\frac{dx}{d\xi} \frac{dm}{d\xi}; \xi] = 0$, then $\frac{1}{2} \frac{dE_N[1; \xi]^2}{d\xi} = 0$, which ensures the local optimality. The case when $\tilde{c} = c$ follows directly by substitution. \square

Note that the approximated moment-matching rule (21) can be implemented as an iterative procedure, where using initial parameters ξ_i , one computes the updated parameters ξ_{i+1} via $\frac{\mathbb{E}_{\theta,N}[\tilde{c}; \xi_i]}{\mathbb{E}_{\theta,N}[1; \xi_i]} = \frac{\partial \psi(\xi_{i+1})}{\partial \xi_{i+1}}$. The update is repeated until the current iterate is close

enough to the fixed point. To analyze the convergence of this iterative procedure, let us denote $\hat{\xi} := \frac{\partial \psi(\xi)}{\partial \xi}$. The mapping from ξ to $\hat{\xi}$ is a diffeomorphism via the Legendre transformation [10, Theorem 2.2.3]. Therefore, we can write $F_N(\hat{\xi}) := \frac{\mathbb{E}_{\theta,N}[\tilde{c}; \hat{\xi}]}{\mathbb{E}_{\theta,N}[1; \hat{\xi}]}$. The approximated moment-matching rule can then be written as a Picard iteration $\hat{\xi}_{i+1} = F_N(\hat{\xi}_i)$. Using Banach's fixed-point theorem, in the proposition below, we show that there exists a fixed point of the mapping F_N on some subset of $\Xi := \{\hat{\xi}: \xi \in \Xi\}$.

Proposition 5. Using the notations of Proposition 4, suppose that for each $\theta \in \Theta$, $\tilde{c}_i(\phi_\xi)u(\phi_\xi)\omega^{-1}$ belongs to $\mathcal{W}_d^r(\mathcal{D})$ for any $i \in \{1, \dots, n_\xi\}$ and for some $r > 0 \in \mathbb{N}$, uniformly for any $\xi \in \Xi_\theta$, where, $\mathcal{W}_d^r(\mathcal{D}) := \{f: \mathcal{D} \rightarrow \mathbb{R}: \|\frac{\partial^{|s|} f}{\partial x_1^{s_1} \dots \partial x_d^{s_d}}\|_\infty < \infty, s_i < r\}$,

with $|s| = \sum_{i=1}^d s_i$ and $\Xi_\theta \subset \Xi$ open. Moreover, assume that $\tilde{c}_i(\phi_\xi)u(\phi_\xi)$ is continuously differentiable in ξ on Ξ_θ . Then there exists an $N_0 \in \mathbb{N}$ and a subset $\hat{\Xi}_c \subset \hat{\Xi}$ such that F_N is a contraction in $\hat{\Xi}_c$ for $N \geq N_0$.

Proof. F_N is continuously differentiable on Ξ_θ by the assumption $\tilde{c}_i(\phi_\xi)u(\phi_\xi)$ is continuously differentiable in ξ on Ξ_θ and the definition of F_N . Using the mean value theorem [17, §0.27] we can write $\|F_N(\hat{\xi}_1) - F_N(\hat{\xi}_2)\| \leq \sup_{\hat{\xi} \in \hat{\Xi}_c} \|\frac{\partial F_N}{\partial \hat{\xi}}\| \|\hat{\xi}_1 - \hat{\xi}_2\|$. Therefore, if $\sup_{\hat{\xi} \in \hat{\Xi}_c} \|\frac{\partial F_N}{\partial \hat{\xi}}\| < 1$ in an open convex subset $\hat{\Xi}_c$ then F_N is a contraction in the set. Notice that using $\frac{\partial \xi}{\partial \hat{\xi}} = (\frac{\partial^2 \psi(\xi)}{\partial \xi^2})^{-1}$ [18, p. 17], we obtain $\frac{\partial F_N}{\partial \hat{\xi}} = (\frac{\partial^2 \psi(\xi)}{\partial \xi^2})^{-1} \frac{\partial F_N}{\partial \xi}$. Since $\{\tilde{c}_i\}$ are linearly independent, then $(\frac{\partial^2 \psi(\xi)}{\partial \xi^2})$ is invertible for any $\xi \in \Xi$ [11]. Therefore, finding $\hat{\Xi}_c$ such that $\sup_{\hat{\xi} \in \hat{\Xi}_c} \|\frac{\partial F_N}{\partial \hat{\xi}}\| < 1$ is equivalent to finding an open convex subset $\Xi_c \subset \Xi_\theta$ such that

$$\sup_{\xi \in \Xi_c} \left\| \left(\frac{\partial^2 \psi(\xi)}{\partial \xi^2} \right)^{-1} \frac{\partial F_N}{\partial \xi} \right\| < 1. \quad (22)$$

Since $\sup_{\xi \in \Xi_c} \|(\frac{\partial^2 \psi(\xi)}{\partial \xi^2})^{-1} \frac{\partial F_N}{\partial \xi}\|$ is less than $\sup_{\xi \in \Xi_c} \|(\frac{\partial^2 \psi(\xi)}{\partial \xi^2})^{-1}\| \sup_{\xi \in \Xi_c} \|\frac{\partial F_N}{\partial \xi}\|$, and, for an invertible matrix T we have $\frac{1}{\|T\|} < \|T^{-1}\|$, condition in (22) is satisfied if $\sup_{\xi \in \Xi_c} \|\frac{\partial F_N}{\partial \xi}\| < \inf_{\xi \in \Xi_c} \|(\frac{\partial^2 \psi(\xi)}{\partial \xi^2})^{-1}\|^{-1} < \inf_{\xi \in \Xi_c} \|(\frac{\partial^2 \psi(\xi)}{\partial \xi^2})\|$. Since Ξ_θ is open, we can select an open subset $\Xi_a \subset \Xi_\theta$ away from the boundary of Ξ such that there exists a positive α satisfying $\alpha I \prec \frac{\partial^2 \psi(\xi)}{\partial \xi^2}$ for any $\xi \in \Xi_a$. This is always possible since $\text{EM}(\tilde{c})$ is a regular exponential family, which means Ξ is an open convex subset of \mathbb{R}^{n_ξ} [9]. Since for any i , $\tilde{c}_i(\phi_\xi)u(\phi_\xi)\omega^{-1} \in \mathcal{W}_d^r(\mathcal{D})$ on Ξ_θ , then $\|F_N(\hat{\xi}(\xi)) - \mathbb{E}_\theta[\tilde{c}]\| = \mathcal{O}(N^{-r} \log(N)^{(d-1)(r-1)})$ on Ξ_θ [19, §4.1.1]. As N approaches infinity, the Jacobian $\frac{\partial F_N}{\partial \xi}$ at any $\xi_a \in \Xi_a$ decreases to zero. Therefore, there exists N_0 and $r_1 > 0$ such that for any $\xi \in B(\xi_a, r_1) \subset \Xi_a$, the requirement $\|\partial F_N / \partial \xi\| < \alpha$ is satisfied for $N \geq N_0$ in $\hat{\Xi}_c := \{\hat{\xi}: \xi \in B(\xi_a, r_1)\}$. \square

The conditions in Proposition 5 can be shown to be satisfied for some $r > 0$ when $|p_\theta(q_\xi^r)|$ is bounded and goes to zero as $\|x\| \rightarrow \infty$ with $\Xi_\theta = \Xi$. This condition is valid for the three numerical simulations considered in Section IV.

C. Second Gaussian-Based Parametric Bijection

In Section III-B, we have used the approximated moment-matching rule (21) to construct the bijection from the hypercube \mathcal{D} to \mathbb{R}^d . However, there are other quadrature methods that do not operate on

the hypercube, for example, the Gauss–Hermite quadrature (GHQ) which operates on \mathbb{R}^d . To compute the cumulant-generating function efficiently using these numerical integration methods, we introduce another bijection where we specifically focus on the GHQ case.

We use $N(d, l)$ to denote the number of quadrature nodes for a dimension d and a level l , such that $N := N(d, l)$. We obtain the sparse multivariate Gauss–Hermite nodes and weights $\{\tilde{x}_i, w_i\}_{i=1}^{N(d, l)}$ by using the Smolyak construction on one-dimensional Gauss–Hermite nodes (see [20] for details). We use a similar choice of univariate quadrature nodes per level as in GPQ, where, for a level $l \in \mathbb{N}$, the corresponding univariate nodes are given by $N(1, l) = 2^{l+1} - 1$. This coincides with the choice of nodes introduced in [21], however in their work, the quadrature levels greater than three are abandoned. Interestingly, if we select $N(1, l) = \mathcal{O}(2^l)$, then both GPQ and GHQ satisfy [16] $N(d, l) = \mathcal{O}(2^l l^{d-1})$.

The exponential of the cumulant-generating function is approximated as follows:

$$\begin{aligned} & \int_{\mathbb{R}^d} \exp(c(x)^\top \theta) dx \\ &= \int_{\mathbb{R}^d} \exp(c(\phi_\xi(\tilde{x}))^\top \theta) \exp(\tilde{x}^\top \tilde{x}) \\ & \quad \times \left| \det \frac{\partial \phi_\xi(\tilde{x})}{\partial \tilde{x}} \right| \exp(-\tilde{x}^\top \tilde{x}) d\tilde{x} \approx \sum_{i=1}^{N(d, l)} w_i z(\tilde{x}_i), \end{aligned} \quad (23)$$

where,

$$\phi_\xi(\tilde{x}) := \mu + \sqrt{2}T^{-1}\Lambda^{1/2}\tilde{x}, \quad (24a)$$

$$z(\tilde{x}) := \exp(c(\phi_\xi(\tilde{x}))^\top \theta) \exp(\tilde{x}^\top \tilde{x}) \left| \det \frac{\partial \phi_\xi(\tilde{x})}{\partial \tilde{x}} \right|. \quad (24b)$$

In (23), $\{\tilde{x}_i\}$ is the set of the Gauss–Hermite quadrature nodes, and $\{w_i\}$ are their corresponding weights. We select μ and Σ according to the moment-matching rule (17). Therefore, the bijection (24a) also ensures that the sparse Gauss–Hermite quadrature nodes are always placed in the high-density domain in \mathbb{R}^d .

The GHQ scheme suffers from a very weak nesting capability since the intersection between roots of Hermite polynomials of successive orders contains only the origin $x = 0$. This is in contrast with the GPQ scheme used in the previous section, which is highly efficient since it has a polynomial exactness up to order $3N + 1$, in addition to being fully nested. Therefore, more integration nodes would be required by GHQ to achieve the same accuracy as GPQ (see [13, Section 3.1.2]). A problem with high-order Gauss–Hermite methods is that the quadrature weights can easily lie below machine precision [22]. In some applications, fortunately, one can ignore the Gauss–Hermite nodes that have weights below machine precision and still obtain satisfying integration results. As we will see in Section IV, with a similar sparse integration level to that of GPQ, the GHQ scheme combined with the adaptive bijection (24a) might offer a competitive advantage compared to GPQ combined with (20) as their quadrature nodes spread wider than those of latter; see Figure 4.

D. Integrating the parametric bijection in the automatic projection filter

We present Algorithm 1 that combines the parametric bijection with the automatic projection filter algorithm. The bijections (20) and (24a) have identical parameters μ and Σ , and thus can be implemented similarly.

IV. NUMERICAL EXAMPLES

In this section, we consider three numerical experiments to assess the effectiveness of our proposed bijections. For these examples, we

Algorithm 1 Single step from the automatic projection filter using parametric bijection.

```

1: procedure AUTOMATICPROJECTIONFILTER( $p_\theta, \theta, \xi, t, dy_t$ )
2:    $g \leftarrow \text{FISHERMETRIC}(p_\theta; \xi)$   $\triangleright$  Calculate Fisher Metric of  $p_\theta$ 
3:    $\tilde{\eta} \leftarrow \text{EXTENDEDEXPECTATION}(p_\theta; \xi)$   $\triangleright$  Calculate
     expectation of the extended natural statistics  $\tilde{c}$ 
4:    $\eta \leftarrow \tilde{\eta}[:m]$   $\triangleright$  The expectation of natural statistics  $c$  is the
     first  $m$  of  $\tilde{\eta}$ 
5:    $d\theta \leftarrow \text{FILTEREQUATION}(g, \xi, \tilde{\eta}, \eta, t, dy_t)$   $\triangleright$  Eq. (9)
6:    $\theta \leftarrow \theta + d\theta$   $\triangleright$  Update the parameter
7:    $\xi \leftarrow \text{UPDATEBIJECTIONPARAMETERS}(\eta, g)$   $\triangleright$  Eq. (21)
8:   return  $\theta, \xi$   $\triangleright$  Return the updated value of the natural
     parameter  $\theta$  and bijection parameter  $\xi$ 
9: end procedure

```

choose \mathcal{P} as the set of polynomials in x_t with order less than or equal to some $n_p \in \mathbb{N}$.

A. Univariate example

The first example is a scalar dynamical system with a nonlinear measurement model [1], [2]:

$$dx_t = \kappa dt + \sigma dW_t, \quad (25a)$$

$$dy_t = \beta x_t^3 dt + dV_t, \quad (25b)$$

with two independent standard Wiener processes $\{W_t, t \geq 0\}$ and $\{V_t, t \geq 0\}$, and three constants given by the process noise constant $\sigma = 0.4$, the drift constant $\kappa = 0.25$, and the nonlinear measurement scale $\beta = 0.8$. It is well known that the optimal filter for this problem is infinite dimensional [23]. We use an exponential manifold with $c_i \in \{x, x^2, x^3, x^4\}$. We remark that the drift term in (25a) makes the filtering problem significantly harder than that of [8]. We choose the initial parameters of the projection filter as $\theta_0 = [0, 2, 0, -1]^\top$. This initial condition vector reflects exactly the initial density of the dynamical system which corresponds to a bimodal non-Gaussian density with peaks at -1 and 1 . We solve the Kushner–Stratonovich stochastic PDE on a uniform grid. The simulation time step is set to be 10^{-4} . We generate one measurement realization with $x_0 = 1$. We compare three different bijections: The first one is a static bijection $\tanh(\tilde{x})^{-1}$, the second one is the Gaussian-based bijection (20), and the third one is the Gauss–Hermite bijection (24a). Furthermore, we use 9 and 18 integration nodes for the static bijection and 9 such nodes for both parametrized bijections.

The simulation results, shown in Figure 2, depict the evolution of the densities obtained with the finite difference approach and with the projection filters, along with their corresponding Hellinger distances, where the Hellinger distance between two densities p and q is given by $\frac{1}{2} \int \mathcal{X}(\sqrt{p} - \sqrt{q})^2 dx$. Even though both projection filters based on parametric bijections (20) and (24a) require less integration nodes than that based on the static bijection, they do however substantially reduce Hellinger distances compared to the finite difference approximation, as shown in Figure 2. The projection filter based on the bijection (20) with GCQ produces better approximated densities than the GHQ scheme across the entire simulation time. This is also shown in Figure 2, where the Hellinger distances associated with the GCQ scheme (FD-vs-Proj-GCQ-9) only oscillate between one and ten times the lowest Hellinger distance obtained from the static bijection with 18 quadrature nodes (FD-vs-static-18). In contrast to this and at the end of the simulation, the Hellinger distance between the finite difference solution and the projection filter approximation using the static bijection with 9 quadrature nodes (FD-vs-static-9) is about one hundred times greater than that from the lowest

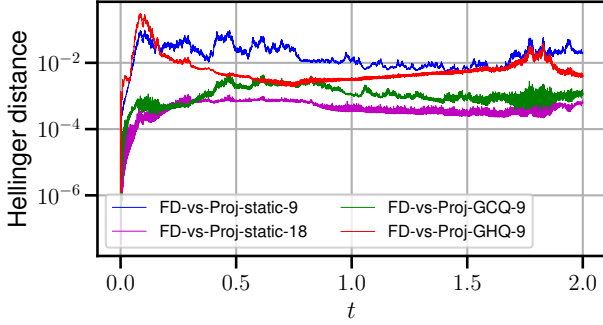


Fig. 2. The Hellinger distances from the finite difference solutions to densities solved by projection filters with static bijections with 9 and 18 nodes (FD-vs-static-9 and FD-vs-static-18), or with parametric bijections (20) and (24a) with 9 nodes, (FD-vs-Proj-GCQ-9 and FD-vs-Proj-GHQ-9), respectively.

Hellinger distance (FD-vs-static-18). Thus, this simulation evidently shows that the parametric bijection (20) is superior to both the static and Gauss–Hermite bijections (24a) for this example which portrays a hard stochastic nonlinear filtering problem to solve.

B. Modified Van der Pol Oscillator

In this section, we compare the projection filter with a bootstrap particle filter with systematic resampling [24]. The dynamic model considered here is a modified Van der Pol oscillator, the standard form of which is widely used as a model for oscillatory processes in physics, electronics, biology, neurology, sociology and economics:

$$\begin{aligned} d \begin{bmatrix} x_{1,t} \\ x_{2,t} \end{bmatrix} &= \begin{bmatrix} \kappa x_{1,t} + x_{2,t} \\ -x_{1,t} + \kappa x_{2,t} + \mu(1 - x_{1,t}^2)x_{2,t} \end{bmatrix} dt + \begin{bmatrix} 0 \\ \sigma_w \end{bmatrix} dW_t, \\ dy &= x_{1,t} dt + \sigma_v dV_t. \end{aligned} \quad (26)$$

In this simulation, we set $\mu = 0.3$, $\kappa = 1.25$, and $\sigma_v = \sigma_w = 1$. We also set the simulation time step to be 2.5×10^{-3} . Unlike the case with $\kappa = 0$, where the probability density evolution can be easily contained using a compact support [8], the probability densities corresponding to (26) with $\kappa > 0$ expand quickly in time. We use here both GPQ and GHQ with their sparse-grid integration schemes where we set the level to four. For the GPQ scheme, the number of nodes used is 129 while for the GHQ scheme, it is 189 after ignoring all nodes with weights less than 10^{-9} . For the particle filter, we use 9.6×10^6 samples in our simulation. We discretize the dynamic model (26) using Euler–Maruyama for both the particle filter and the measurement process. For a multi index $\underline{i} \in \mathbb{N}^2$, define $x^{\underline{i}} = x_1^{i(1)} x_2^{i(2)}$. The natural statistics are set to be $x^{\underline{i}}$, where $1 \leq |\underline{i}| \leq 4$. Further, the initial density is set to be the standard Gaussian density. To show the performance of the projection filter obtained by both sparse integration schemes, we calculate the empirical densities of the particle filter on a fixed grid. The comparison of the empirical densities from the particle filters with those from the projection filters is shown in Figure 4, while the Hellinger distances between the empirical densities and those from the projection filters are in Figure 3. Figure 4 shows that the bjected quadrature nodes of both sparse GPQ and GHQ schemes are systematically adapting to the shapes of the densities as they evolve in time. The shapes of the projection densities resemble those of the empirical densities from the particle filter, except that the projection filter's densities cannot capture some sharp notch-like shapes with low values as in Figure 4. The Hellinger distances from the projection filter's densities obtained using the GHQ scheme to the empirical

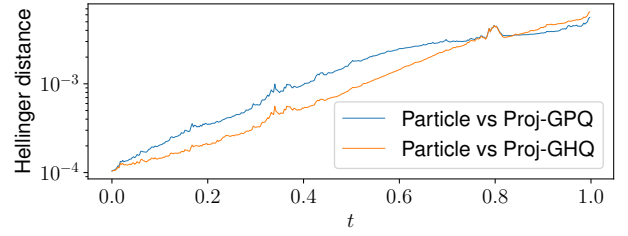


Fig. 3. Hellinger distance from the empirical densities to the projection filter's densities solved using both GPQ and GHQ.

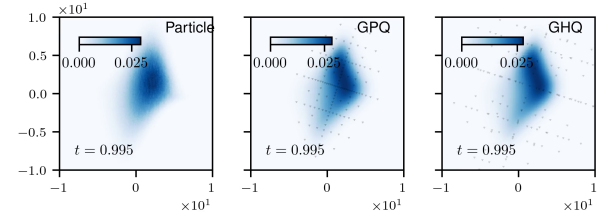


Fig. 4. Comparison of empirical densities from particle filter (left) and densities from the projection filters solved using GPQ (center) and GHQ (right) at $t = 0.995$. The grey dots represents the position of the bjected quadrature nodes of the sparse Gauss–Patterson or Gauss–Hermite schemes, respectively.

densities are slightly lower compared to those obtained using the GPQ scheme.

Table I shows computational times of the projection filter with different sparse-grid levels and adaptive bijections, and the projection filter with a static bijection. For the static bijection, we use Gauss–Patterson sparse grid integration, where we set the static bijection to be \tanh^{-1} following [8]. As can be seen, the execution time of the projection filter using GHQ level 4 with bijection (24a) is the fastest compared to the other projection filter schemes. We found that even with the maximum sparse-grid level available for Gauss–Patterson sparse grid integration (level 8), the projection filter with static bijection produces ill-defined projection densities around $t = 0.7$. Therefore, to accurately implement the projection filter using the static bijection, a sparse-grid level higher than 8 is necessary, which means a significant increase in the quadrature nodes that will result in a substantial rise in execution time. As shown in Table I, the computational times for the GHQ with bijection (24a) increase only modestly, compared to those of the GPQ with bijection (20).

TABLE I
COMPUTATION TIME COMPARISON FOR SECTION IV.B

Scheme	Level				
	4	5	6	7	8
GPQ	3.543s	3.678s	4.012s	4.785s	6.315s
GHQ	1.619s	1.636s	1.674s	1.833s	1.961s
static-GPQ	-	-	-	-	1.964s

C. Stochastic Epidemiology Application

In this section, we consider an application of the projection filter to the stochastic suspected infected or recovery (SIR) nonlinear filtering problem, widely used for example in the study of the spread of

infectious diseases. Consider the following SDE [25]:

$$\begin{aligned} d \begin{bmatrix} x_{1,t} \\ x_{2,t} \end{bmatrix} &= \begin{bmatrix} -\beta x_{1,t} x_{2,t} - \mu x_{1,t} + \mu \\ \beta x_{1,t} x_{2,t} - (\lambda + \mu) x_{2,t} \end{bmatrix} dt + \begin{bmatrix} -\sigma x_{1,t} x_{2,t} \\ \sigma x_{1,t} x_{2,t} \end{bmatrix} dW_t, \\ dy_{1,t} &= x_{2,t} dt + k dV_t. \end{aligned} \quad (27)$$

In this equation, $x_{1,t}$ is the fraction of the suspected population, $x_{2,t}$ is the fraction of the infected population, assuming that the population size is constant. The fraction of the recovered population is given by $1 - (x_{1,t} + x_{2,t})$, and its dynamic is non-stochastic which can be excluded from the SDE. The constants β, μ, λ correspond to the average number of contacts per infection per day, the birth rate, and the recovery rate of the infected people, respectively. The constants σ , and k are positive constants associated with the process and measurement noises, respectively.

If $0 < \beta < \min(\lambda + \mu - \frac{\sigma^2}{2}, 2\mu)$ then the disease-free equilibrium $x_* = (1, 0)$ is globally asymptotically stable [25, Theorem 2.1]. Therefore, the stationary probability measure has no density with respect to the Lebesgue measure. The high-density domain of the conditional probability density of SIR dynamics will be shrinking in time. In our simulation, we chose $\mu = 0.2, \beta = 0.14, \lambda = 0.1, \sigma = 0.2, k = 10^{-4}$ and set the initial density to be a Gaussian density with mean $[0.95, 0.02]^T$ and variance $\text{diag}[0.95, 0.02] \times 10^{-3}$. Using a similar exponential family to that of the previous section, we compare here the performance of the projection filter achieved by using the bijection (20) and GPQ level 5 with that of the particle filter. The Hellinger distance between the two densities at different times can be seen in Figure 5. This, therefore, clearly shows that the bijection (20) can also perform very well in accurately tracking probability densities that shrink in time, as is the case here with SIR dynamics, and, by the same token, also demonstrates the adaptive capability of the proposed bijection (20). Compared to the projection filter with the proposed bijections, employing the projection filter alongside GPQ level 8 and the static bijection \tanh^{-1} leads to an ill-defined projection density within just a few iterations.

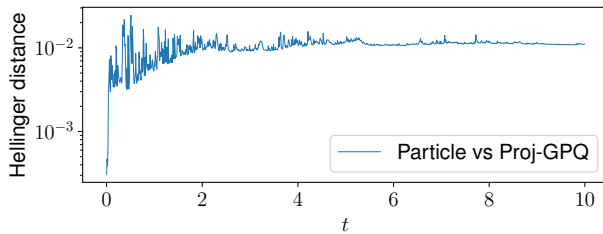


Fig. 5. Hellinger distance from the empirical densities to the projection filter's densities solved using GPQ level 5.

V. CONCLUSIONS

In this work, we have introduced two new parametric bijections for the automatic projection filter that was recently proposed in [8]. The first bijection was constructed by selecting a Gaussian density q_ξ whose parameters were obtained by minimizing the KL divergence between the projected density p_θ and the Gaussian density q_ξ , which is equivalent to evaluating moment-matching conditions. We have shown that this bijection also minimizes the squared integration error under some sufficient theoretical conditions. The second bijection was also constructed via the same moment-matching conditions, but it was tailored for the GHQ scheme. We then applied these bijections to three practically-motivated numerical examples, and we found that they all achieved superior performance in terms of the Hellinger distances to the ground truth than the static bijection, using fewer quadrature nodes and thus achieving both higher accuracy and reduced computational time.

REFERENCES

- [1] B. Hanzon and R. Hut, "New results on the projection filter," in *European Control Conference*, Grenoble, Jul. 1991, p. 9.
- [2] D. Brigo, B. Hanzon, and F. L. Gland, "Approximate nonlinear filtering by projection on exponential manifolds of densities," *Bernoulli. Official Journal of the Bernoulli Society for Mathematical Statistics and Probability*, vol. 5, no. 3, p. 495, Jun. 1999.
- [3] H. J. Kushner, "On the differential equations satisfied by conditional probability densities of Markov processes, with applications," *Journal of the Society for Industrial and Applied Mathematics, Series A: Control*, vol. 2, no. 1, pp. 106–119, 1964.
- [4] J. Armstrong and D. Brigo, "Nonlinear filtering via stochastic PDE projection on mixture manifolds in L^2 direct metric," *Mathematics of Control, Signals, and Systems*, vol. 28, no. 1, p. 5, Dec. 2016.
- [5] J. Armstrong, D. Brigo, and B. Hanzon, "Optimal projection filters with information geometry," *Info. Geo.*, Jun. 2023.
- [6] S. Koyama, "Projection smoothing for continuous and continuous-discrete stochastic dynamic systems," *Signal Processing*, vol. 144, pp. 333–340, Mar. 2018.
- [7] A. Kutschireiter, L. Rast, and J. Drugowitsch, "Projection Filtering with Observed State Increments with Applications in Continuous-Time Circular Filtering," *IEEE Transactions on Signal Processing*, vol. 70, pp. 686–700, 2022.
- [8] M. F. Emzir, Z. Zhao, and S. Särkkä, "Multidimensional projection filters via automatic differentiation and sparse-grid integration," *Signal Processing*, vol. 204, p. 108832, Mar. 2023.
- [9] L. D. Brown, "Fundamentals of Statistical Exponential Families with Applications in Statistical Decision Theory," *Lecture Notes-Monograph Series*, vol. 9, pp. i–279, 1986.
- [10] R. E. Kass and P. W. Vos, *Geometrical Foundations of Asymptotic Inference*, ser. Wiley Series in Probability and Statistics. New York: Wiley, 1997, "A Wiley Interscience publication."
- [11] O. Calin and C. Udriște, *Geometric Modeling in Probability and Statistics*. Springer International Publishing, 2014.
- [12] D. Brigo, "Optimal Projection Filters," May 2022, comment: arXiv admin note: text overlap with arXiv:1610.03887.
- [13] W. Gautschi, *Orthogonal Polynomials: Computation and Approximation*, ser. Numerical Mathematics and Scientific Computation. Oxford New York: Oxford university press, 2004.
- [14] R. T. Rockafellar, *Convex Analysis*, ser. Princeton Mathematical Series. Princeton, N.J: Princeton University Press, 1970, no. 28.
- [15] R. Herbrich, "Minimising the Kullback–Leibler Divergence," Microsoft, Tech. Rep., 2005.
- [16] T. Gerstner and M. Griebel, "Numerical integration using sparse grids," *Numerical Algorithms*, vol. 18, no. 3/4, pp. 209–232, 1998.
- [17] T. Aubin, *A Course in Differential Geometry*, ser. Graduate Studies in Mathematics. Providence, R.I: American Mathematical Society, 2001, no. v. 27.
- [18] S.-i. Amari, *Information Geometry and Its Applications*, ser. Applied Mathematical Sciences. Tokyo: Springer Japan, 2016, vol. 194.
- [19] M. Holtz, *Sparse Grid Quadrature in High Dimensions with Applications in Finance and Insurance*, ser. Lecture Notes in Computational Science and Engineering. Heidelberg New York: Springer, 2011, no. 77.
- [20] H.-J. Bungartz and M. Griebel, "Sparse grids," *Acta Numerica*, vol. 13, pp. 147–269, May 2004.
- [21] B. Jia, M. Xin, and Y. Cheng, "Sparse Gauss-Hermite Quadrature Filter with Application to Spacecraft Attitude Estimation," *Journal of Guidance, Control, and Dynamics*, vol. 34, no. 2, pp. 367–379, Mar. 2011.
- [22] L. N. Trefethen, "Exactness of Quadrature Formulas," *SIAM Review*, vol. 64, no. 1, pp. 132–150, Feb. 2022.
- [23] M. Hazewinkel, S. I. Marcus, and H. J. Sussmann, "Nonexistence of finite-dimensional filters for conditional statistics of the cubic sensor problem," *Systems & Control Letters*, vol. 3, no. 6, pp. 331–340, Dec. 1983.
- [24] N. Chopin, *An Introduction to Sequential Monte-Carlo*. Cham, Switzerland: Springer, 2020.
- [25] E. Tornatore, S. Maria Buccellato, and P. Vetro, "Stability of a stochastic SIR system," *Physica A: Statistical Mechanics and its Applications*, vol. 354, pp. 111–126, Aug. 2005.

Supplementary Materials for *Gaussian-Based Parametric Bijections For Automatic Projection Filters*

Muhammad Emzir, Zheng Zhao, Lahouari Cheded, Simo Särkkä

I. INTRODUCTION

In this supplementary documentation, in Table I, we give the essential notations employed in the main paper. Alongside this, we offer supplementary plots that augment the paper's content.

II. NOTATIONS

TABLE I
LIST OF IMPORTANT NOTATIONS USED IN THE PAPER.

Variable	Description
d	Dimension of the stochastic dynamics' state.
d_y	Dimension of the measurement vector.
\mathcal{D}	Canonical hypercube, $(-1, 1)^d$.
erf	Error-function.
\mathbb{E}	Expectation operator.
$\mathbb{E}_{\theta, N} [f; \xi]$	Approximated expectation of an arbitrary function f under a parametric density p_θ via the numerical quadrature $Q_N^{d, \omega}$.
$\text{EM}(c)$	Set of all exponential density functions with natural statistics c , $\{p \in \mathcal{P} : p(x) = \exp(c(x)^\top \theta - \psi(\theta))\}$.
$\text{KL}(p q)$	Kullback-Leibler divergence between two densities, p and q .
\mathcal{L}	Backward diffusion operator.
m	Number of natural parameters.
\mathcal{P}	Class of probability density functions with respect to the standard Lebesgue measure on \mathcal{X} .
$Q_N^{d, \omega} f$	d -dimensional numerical quadrature of a function f with a positive weight function $\omega(\tilde{x})$ and N quadrature nodes.
Q_t, R_t	Invertible spectral density matrices of W_t and V_t , at $t \geq 0$, respectively.
\mathcal{S}	Class of parametric densities.
W_t, V_t	Independent Wiener processes taking values in \mathbb{R}^{d_w} and \mathbb{R}^{d_y} , respectively.
$\mathcal{W}_d^r(\mathcal{D})$	Space of functions with bounded mixed partial derivatives up to order s ; i.e., $\mathcal{W}_d^r(\mathcal{D}) := \{f : \mathcal{D} \rightarrow \mathbb{R} : \ \frac{\partial^{ s } f}{\partial \tilde{x}_{(1)}^{s_1} \dots \partial \tilde{x}_{(d)}^{s_d}}\ _\infty < \infty, s_i < r\}$.
x	State of the dynamics.
\mathcal{X}	Space of all possible states.
\mathcal{Y}	Space of all possible measurements.
θ	Natural parameters.
Θ	Set of all natural parameters.
ϕ	Fixed smooth bijection $\mathcal{D} \rightarrow \mathcal{X}$.
ϕ_ξ	Parametrized smooth bijection $\mathcal{D} \rightarrow \mathcal{X}$ with parameters ξ .
$\psi(\theta)$	Cumulant-generating function at θ w.r.t $\text{EM}(c)$.

III. ADDITIONAL PLOTS

A. Univariate Problem in Section IV.A

Figure 1 illustrates a comparison between conditional densities derived from solving Kushner–Stratonovich SPDEs using the finite difference method (considered the ground truth) and those computed using the projection filter at different time points. This figure, similar to the Hellinger distance plot (Figure 2 in the paper), displays the similarity between the conditional densities approximated by the projection filter, utilizing Gauss–Chebyshev numerical integration and bijection (20) (Proj-GCQ-9), and the finite difference solutions to the Kushner–Stratonovich equation (FD). Qualitatively, the densities Proj-GCQ-9 are comparable to the approximated conditional densities generated by the projection filter with a static bijection and twice the quadrature nodes (Proj-Static-18).

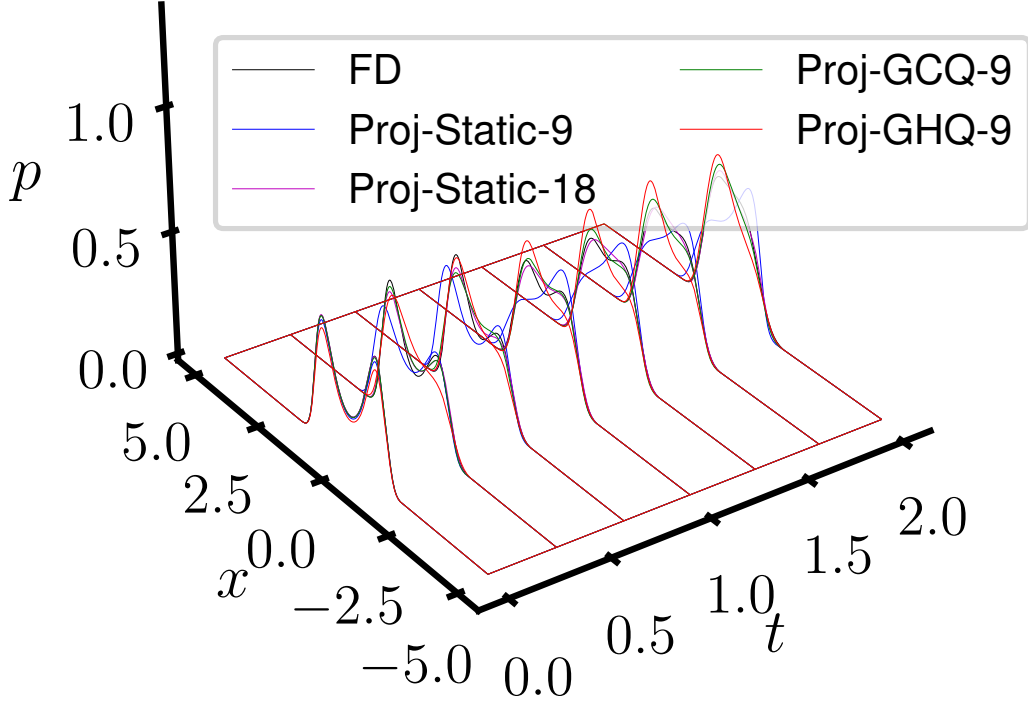


Fig. 1. This figure shows a comparison between the densities obtained by employing finite difference schemes (represented in black), densities obtained through the application of projection filters using a static bijection with 9 and 18 quadrature nodes and densities obtained from solving projection filters utilizing the bijections provided in formulas (20) and (24a) (depicted in blue and magenta respectively).

B. Bivariate Problem in Section IV.B

Figure 2 shows that even with the maximum sparse-grid level available for Gauss–Patterson sparse grid integration (level 8), the projection filter with static bijection produces an ill-defined projection densities around $t = 0.7$, which is reflected in the explosive Hellinger distance between the empirical densities from the particle filter and the densities obtained via the projection filter with the static bijection. Therefore, to accurately implement the projection filter using the static bijection, a sparse-grid level higher than 8 is necessary, which means a significant increase in the quadrature nodes that will result in a substantial rise in execution time.

Figure 4 shows a comparison of moments calculated through partial differentiation of the cumulant-generating function using the projection filter algorithm and those derived from the particle filters, which are considered the ground truth. Notably, the moments obtained from GHQ exhibit a closer correspondence with the particle filter’s moments than those derived from GPQ. These plots also show corresponding polynomial functions of state realizations for illustrative purposes.

C. Bivariate Problem in Section IV.C

The computational times for the numerical example in Section IV.C exhibit similarity to those in Section IV.B, as both involve bivariate dynamics. It is, however, crucial to highlight that in the numerical example outlined in Section IV.C, employing the projection filter alongside GPQ level 8 and the \tanh^{-1} static bijection leads to an ill-defined projection density within a few iterations (see Figure 3). This observation implies that for this specific optimal filtering problem, the usage of Gauss–Patterson sparse-grid quadrature with the static bijection \tanh^{-1} demands a higher level of sparse-grid integration compared to that in Section IV.B. Consequently, this level would result in an increase in computational time. This also emphasizes the efficiency of the two proposed bijections in this paper, as employing these bijections along with sparse-grid quadrature enables seamless operation of the projection filter.

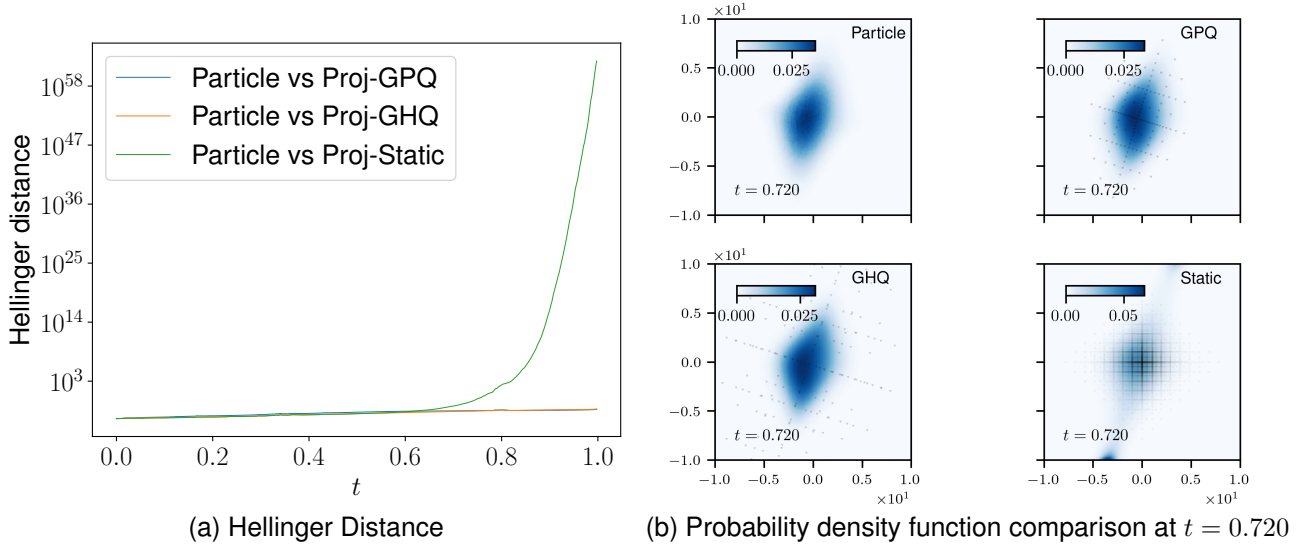


Fig. 2. Figure 2a shows a comparison of Hellinger distances between the empirical densities of the particle filter and the projection filter densities obtained through adaptive and static bijections. In Figure 2b, it is obvious that starting from $t = 0.72$, the projection densities calculated using the static bijection \tanh^{-1} and Gauss–Patterson sparse-grid quadrature level 8 begin to deviate significantly from the empirical densities of the particle filter. The deviations appear since significant portions of high-density regions moved outside the quadrature node locations.

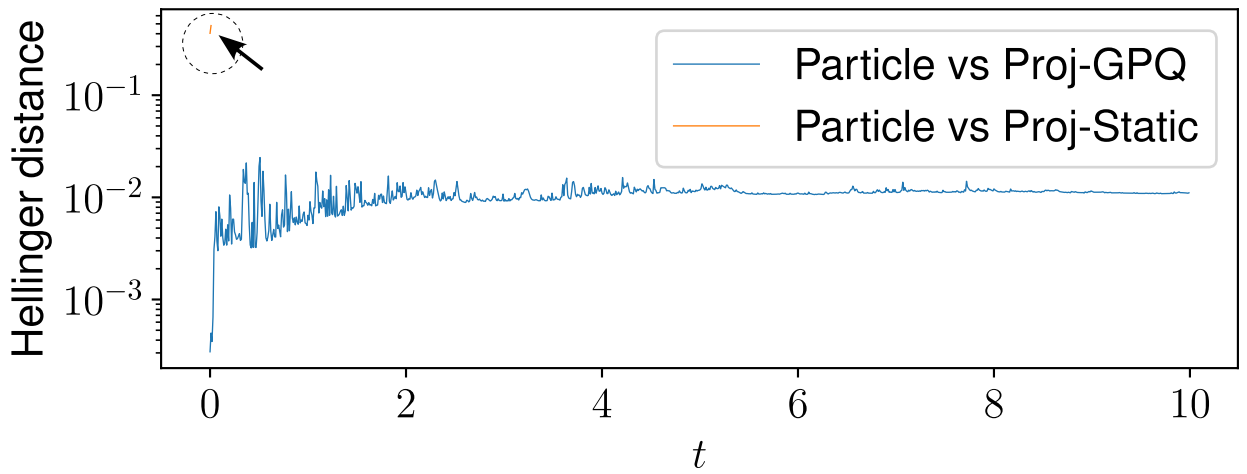


Fig. 3. Hellinger distance from the empirical densities to the projection filter's densities solved using GPQ level 5 with bijection (20), and GPQ level 8 with \tanh^{-1} static bijection. The projection filter with the static bijection leads to an ill-defined projection density within just a few iterations (see the black arrow).

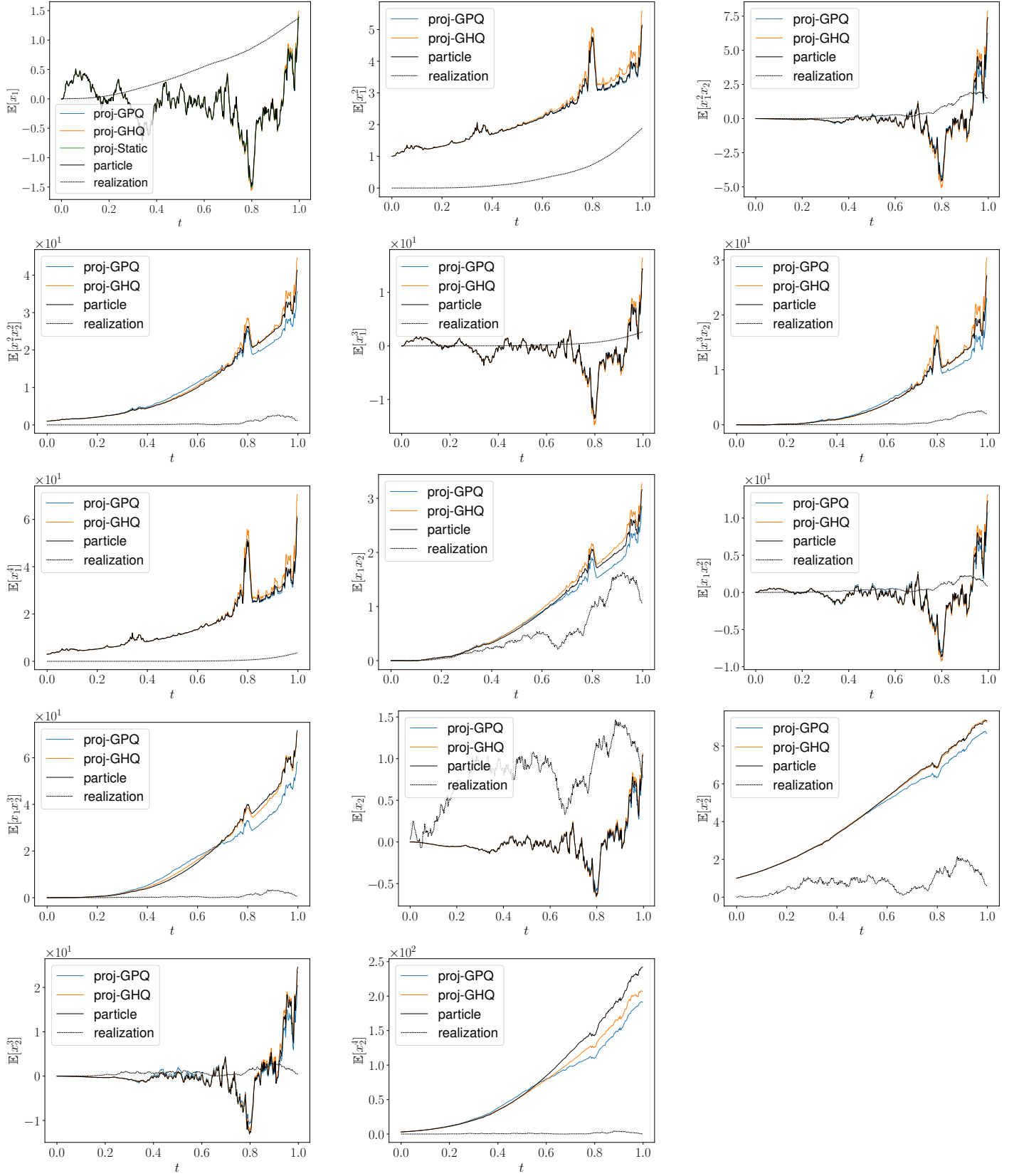


Fig. 4. Comparison approximation of natural statistic's expected values solved by the projection filter and the particle filter.